Peak position of dissipation spectrum in turbulent boundary layers

Yoshiyuki Tsuji
Department of Energy Engineering and Science, Nagoya University, Nagoya 464-8603, Japan
(Received 24 November 1998)

The peak locations of energy dissipation spectrum (y_{kp}^+) are investigated experimentally in the low Reynolds number ($R_\theta < 5000$) zero-pressure-gradient turbulent boundary layers. These peaks are scaled by the relation $y_{kp}^+ = 2(u_* \delta/\nu)^{1/2} = 2R_*^{1/2}$, where u_* is friction velocity and δ is the boundary layer thickness. They are located close to the peak positions of the Reynolds shear stress (y_p^+), that is, $y_{kp}^+ \simeq y_p^+$. This result predicts that the small-scale structures residing in high-energy dissipation regions concentrate around y_p^+.
[S1063-651X(99)01806-1]

PACS number(s): 47.15.−x

I. INTRODUCTION

In this short paper we consider the peak wave number of the dissipation spectrum k_p near the wall region in zero-pressure-gradient boundary layers. Much attention has been paid recently to the small-scale structures wrapped by the high-vorticity concentration regions, which tend to form tubelike or sheetlike structures [1,2]. These diameters and lengths are estimated to be on the order of Kolmogorov length scale and integral scale, respectively. Significant information is contained in the wave-number k_p to consider the small coherent vortex dynamics.

From the empirical knowledge obtained by analyzing many experimental data, She and Jackson predicted that the energy spectrum is dominated by an approximate k^{-1} law over the $k^{-5/3}$ law around the wave number of k_p [3]. They consider a spectrum flatter than $-\frac{5}{3}$ to reflect the coherent vortex dynamics occurring around $k \simeq k_p$. This is confirmed by the numerical simulation of Jiménez *et al.* [1], who reported that the local energy spectrum where the flow includes the vortex tubes displays k^{-1} behavior, while the global spectrum is consistent with $k^{-5/3}$. Passot *et al.* [2] also discussed this problem and found from their numerical data that a $k^{-5/3}$ spectrum develops following larger wave numbers by a k^{-1} range, and the transition occurs close to the Taylor wave number.

We investigate the zero-pressure-gradient boundary layers, and discuss the peak wave number of dissipation spectra close to the wall, which seem to be a key factor while thinking about the small-scale structures. Finally, the relation between the peak locations of dissipation spectra and those of Reynolds shear stress will be discussed.

II. EXPERIMENTAL CONDITION

A typical two-dimensional turbulent boundary layer is developed on a flat plate with zero-pressure gradient in a wind tunnel with a test section 0.32×1.06 m^2 in area and 2.6 m in length. The measured fluctuation velocity in a free stream region is smaller than 0.3%. A tripping wire of 1 mm in diameter is placed 50 mm downstream of the leading edge and adjusted carefully to minimize flow asymmetry. The experimental data are measured at 1900 mm downstream from the leading edge by means of both *I* probe and *X* probe. The *I* probe is made of tungsten wire with the sensor length, $l_s \simeq 0.5$ mm, and its diameter is $\phi = 3.1$ μm. The *X* probe has the dimensions $l_s = 1.0$ mm and $\phi = 5.0$ μm. Velocity signals were sampled by a 12-bit A/D converter with sampling frequency 100 and 50 kHz.

Typical flow characteristics, such as a free streamwise velocity U_0, a friction velocity u_*, a momentum thickness θ, the Reynolds number based on the momentum thickness, and the Reynolds number defined as $R_* \equiv u_* \delta/\nu$, are summarized in Table I.

III. PEAK POSITIONS OF DISSIPATION SPECTRA

We shall consider the energy dissipation field close to the wall. The wave-number k_p at the peak position of the dissipation spectrum is defined as

$$\frac{\partial}{\partial k_1}\{D(k_1)\}|_{k_1=k_p} = 0, \quad D(k_1) \equiv k_1^2 E_{11}(k_1), \tag{1}$$

TABLE I. Typical characteristics of the boundary layers.

No.	U_0	u_*	θ	R_θ	R_*	l_s/ϕ
(a) Experimental results of *I*-probe measurements						
DI1	5.48	0.244	3.88	1364	596	167
DI2	8.76	0.371	3.82	2149	905	167
DI3	12.04	0.439	3.82	2913	1141	167
DI4	15.32	0.616	3.54	3481	1346	167
DI5	18.73	0.739	3.48	4167	1604	167
DI6	4.57	0.203	4.47	1413	560	137
DI7	7.62	0.321	4.23	2227	822	137
DI8	10.69	0.439	3.88	2862	1056	137
DI9	13.78	0.555	3.60	3426	1264	137
DI10	11.83	0.486	3.79	2799	1032	146
DI11	15.21	0.611	3.72	3533	1296	146
DI12	18.59	0.734	3.60	4175	1465	146
DI13	21.98	0.857	3.44	4710	1658	146
(b) Experimental results of *X*-probe measurements						
DX1	5.32	0.237	3.76	1324	627	200
DX2	8.58	0.368	3.37	1897	869	200
DX3	12.49	0.479	3.21	2483	1096	200

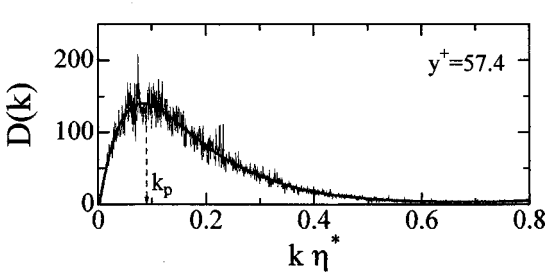

FIG. 1. Typical example of the energy dissipation spectrum, the horizontal axis is normalized by $\eta^*[\eta^* \equiv (\nu/\varepsilon^*)^{1/4}]$. The solid line is the 9th-order polynomial fit.

where $E_{11}(k_1)$ is the one-dimensional energy spectrum in the streamwise direction and k_1 is the wave number. Only the streamwise component is considered in this report, so the wave number is expressed as k instead of k_1, and we call $D(k)$ the dissipation spectrum. Using Taylor's frozen flow hypothesis and the isotropic relation, energy dissipation can be computed as

$$\varepsilon^* = 15\nu \int_0^\infty D(k_1)dk_1 = 15\nu\langle(\partial u/\partial x)^2\rangle. \tag{2}$$

This is called a one-dimensional surrogate. As it is difficult to determine the k_p value accurately, the dissipation spectrum was approximated by the 9th-order polynomial [4], and the peak position was then obtained from it (see Fig. 1).

The previous experimental results [3–5] have shown that the following relation holds:

$$k_p\eta \simeq 0.1, \tag{3}$$

where η is the Kolmogorov length defined as $\eta \equiv (\nu^3/\varepsilon)^{1/4}$ and ε is the dissipation rate per unit mass. If Kolmogorov's assumption (1941) is completely true, the ratio $k_p\eta$ would have a unique value independent of the Reynolds number based on the Taylor microscale R_λ. However, this ratio $k_p\eta$ may be a weak function of R_λ because of the small-scale intermittency in the velocity field. At this stage the experimental accuracy is not enough to reveal that functional relation. The typical results of $k_p\eta^*$ $[\eta^* \equiv (\nu/\varepsilon^*)^{1/4}]$ are plotted against the distance from the wall in Fig. 2. In the outer region, $0.2 < y/\delta < 0.7$, the ratio satisfies Eq. (3), but in the inner region defined here for convenience as $15 < y^+ < 100$, it follows the relation,

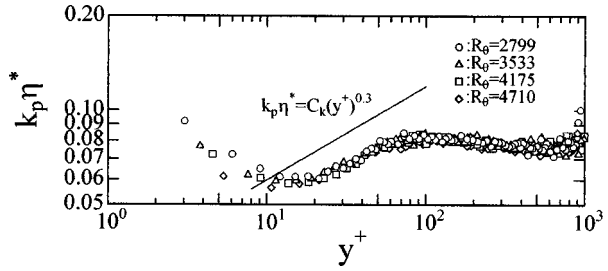

FIG. 2. The product of the peak wave number and the Kolmogorov length scale is plotted against the distance from the wall. The solid line indicates Eq. (4).

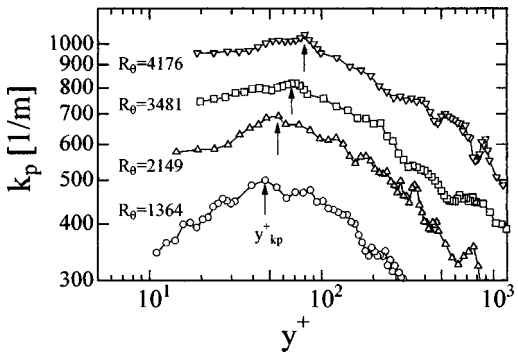

FIG. 3. The peak wave-number distribution for different Reynolds numbers. The arrows indicate the maximum location.

$$k_p\eta^* = C_k(y^+)^\alpha, \tag{4}$$

where C_k and α are constants. There is no necessity to satisfy Eq. (3) in the near wall region because the Kolmogorov scale η depends only on ε and ν; however k_p is representative of small-scale coherent vortexes.

The peak wave-number k_p is obtained at each measuring position, and they are plotted as a function of the distance from the wall in Fig. 3. In each Reynolds number, there is a peak location at some distance from the wall. Here, we define this as y^+_{kp} (see arrows in the graph). It is clear from the graph plotted in Fig. 4 that y^+_{kp} is a function of Reynolds number. The solid line indicates the following relation,

$$y^+_{kp} = 2R_*^{1/2}. \tag{5}$$

Although there is scatter, this equation can predict the distribution of y^+_{kp}. The inset shows the local mean velocity at y^+_{kp}. The ratio is almost constant $U(y^+_{kp})/U_0 = 0.62$ independent of the Reynolds number. These features are very similar to the peak locations of the Reynolds shear stress y^+_p; thus, we will discuss these peaks in Sec. IV.

We try to evaluate the dissipation rate normalized by the inner variables by the following relation,

$$\varepsilon^+ = \varepsilon\nu/u_*^4 = d_1(y^+)^{-d_2}, \quad \varepsilon = \nu\left\langle \frac{\partial u_j}{\partial x_i}\left(\frac{\partial u_i}{\partial x_j} + \frac{\partial u_j}{\partial x_i}\right)\right\rangle, \tag{6}$$

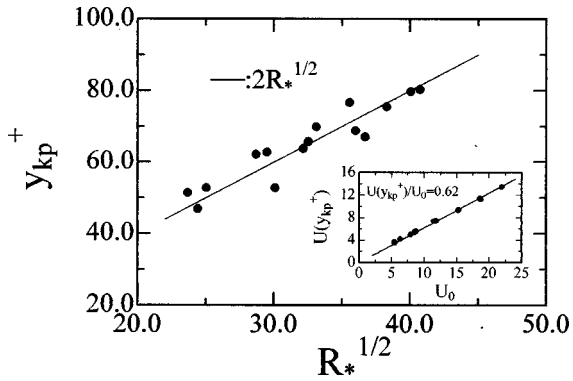

FIG. 4. The relation between the peak position of the energy dissipation spectrum and Reynolds number. Inset figure indicates the local mean velocity at y^+_{kp}.

by means of the experimental and numerical data reported by Klebanoff ($R_\theta \sim 8000$) [6], Honkan and Andreopoulos ($R_\theta = 2790$) [7], Balint, Wallace, and Vukoslavčević ($R_\theta = 2685$) [8], and Spalart ($R_\theta = 1410$) [9]. The dissipation rate can be scaled in the inner region by Eq. (6); the exponents are $d_1 \simeq 4.2$ and $d_2 \simeq 1.1$, respectively. A further simplification can be made by the local isotropy assuming Taylor's frozen flow hypothesis by Eq. (2). However, the evaluation of ε^* cannot be correct close to the wall, that is, $\varepsilon \neq \varepsilon^*$. Our experimental data indicate that the spatial derivative of streamwise velocity, which is normalized by the inner variables, is scaled by the relation; $\langle (\partial u^+/\partial x^+)^2 \rangle = d_3 (y^+)^{-d_4}$ with $d_3 \simeq 0.03$ and $d_4 \simeq 0.8$ for $y^+ < 200$. Then the difference between Eq. (2) and Eq. (6) is significant close to the wall. In this paper, we assume the inner scaling for both ε^+ and $\langle (\partial u^+/\partial x^+)^2 \rangle$ is appropriate, and the exponents d_2 and d_4 are used in the following analysis.

IV. RESULTS AND DISCUSSION

We have discussed the scaling of y_{kp}^+ and the ratio $U(y_{kp}^+)/U_0$ against the Reynolds number R_*. These results are very similar to the feature of the peak locations for the Reynolds shear stress (y_p^+) reported so far. The peak positions y_p^+ are scaled by the empirical relation, $y_p^+ = C_1 R_*^{1/2}$, and the velocity ratio is $U(y_p^+)/U_0 = C_2$, where C_1 and C_2 are constants. The value of C_1 was obtained by Long and Chen [10] and by Sreenivasan [11] independently, at 1.87 and 2, respectively. Simpson reported $C_2 = 0.63$ [12], while Sreenivasan obtained 0.65 [11,13]. Therefore, at least for the low Reynolds number flows ($R_\theta < 5000$), the experimental results assume the relation $y_p^+ \simeq y_{kp}^+$.

It might seem somewhat curious that these two points are located at almost the same position from the wall. The curious feature arises because the Reynolds shear stress is believed to be the representative of large scale, while the energy dissipation is associated with the smallest scale. Some discussion of the result $y_p^+ \simeq y_{kp}^+$ is given below.

The turbulence energy equation derived from the boundary layer equation shows that in the inner region except close to the wall, the advection term can be neglected and the production term balances the dissipation term. In the two-dimensional boundary layer, this means, approximately,

$$-\langle uv \rangle \frac{dU}{dy} \simeq \varepsilon. \tag{7}$$

The local isotropic relation enables us to obtain ε^* instead of ε. But the difference is significant close to the wall; so, the following function is introduced,

$$\varepsilon^*/\varepsilon = f(y^+), \quad \eta^*/\eta = f(y^+)^{-1/4}, \tag{8}$$

where $f(y^+)$ can be expressed by the empirical scaling form and the exponent discussed in Sec. III as

$$f(y^+) = 15(d_3/d_1)(y^+)^{d_2 - d_4}. \tag{9}$$

The peak location y_{kp}^+ is contained in the lower log-law region, so the empirical result of Eq. (4) allows us to obtain the following relation:

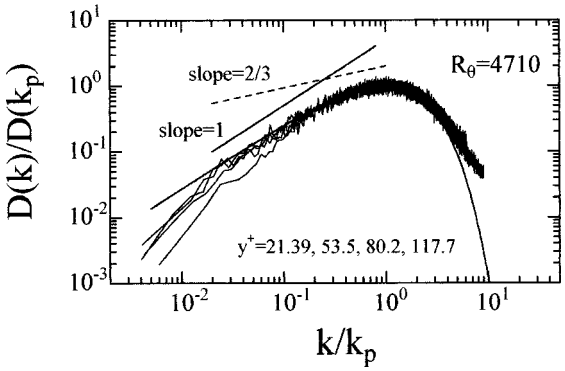

FIG. 5. The normalized dissipation spectrum by the peak wave-number k_p and the spectrum level at k_p. The solid line indicates Eq. (13).

$$-\langle uv \rangle \simeq \frac{\kappa y}{u_*}\left(\frac{\nu^3}{\eta^4}\right) = \frac{\kappa y^+}{u_*^2}\left\{\frac{\nu^4 f(y^+)}{(C_k y^{+\alpha}/k_p)^4}\right\} = \frac{\kappa}{C_k^4}\left(\frac{\nu^2}{u_*}\right)^2 k_p^4 (y^+)^{1-4\alpha+d_2-d_4}(15 d_3/d_1). \tag{10}$$

The value of the exponent α defined in Eq. (4) is not clear. However, experimental data, indicated by a solid line in the inset of Fig. 2, suggest that $\alpha \simeq 0.3$. In this case, when both sides of Eq. (10) are differentiated with respect to the distance from the wall,

$$\frac{\partial}{\partial y^+}\left(\frac{-\langle uv \rangle}{u_*^2}\right) = \frac{\partial}{\partial y^+}\left\{\frac{\kappa}{C_k^4}\left(\frac{15 d_3}{d_1}\right)\left(\frac{\nu}{u_*}\right)^4 k_p^4\right\} = 4\frac{\kappa}{C_k^4}\left(\frac{15 d_3}{d_1}\right)\left(\frac{\nu}{u_*}\right)^4 k_p^3\left(\frac{\partial k_p}{\partial y^+}\right), \tag{11}$$

If there is a peak position in the shear stress profile, that means

$$\left.\frac{\partial}{\partial y^+}\left(\frac{-\langle uv \rangle}{u_*^2}\right)\right|_{y^+ = y_p^+} = 4\frac{\kappa}{C_k^4}\left(\frac{15 d_3}{d_1}\right)\left(\frac{\nu}{u_*}\right)^4 k_p^3\left(\frac{\partial k_p}{\partial y^+}\right)_{y^+ = y_{kp}^+} = 0 \Leftrightarrow y_p^+ = y_{kp}^+. \tag{12}$$

Therefore, the peak location of the shear stress matches that of the dissipation spectrum.

In Fig. 5 the dissipation spectra collapse when scaled by the wave-number k_p of peak dissipation and also by the spectrum level at k_p. In the inner region all the spectra scaled well by a single curve,

$$D(k)/D(k_p) = \beta(k/k_p)\exp(-\gamma k/k_p), \tag{13}$$

where the coefficients are obtained uniquely under the condition that the dissipation spectrum peaks at $k = k_p$; thus, $\beta = e = 2.7182\ldots$ and $\gamma = 1$. The existence of an inverse power-law region for the streamwise velocity component in wall-bounded shear flows has been noted in the literature before [see, for example, Refs. [11] and [14]]. Such a power law can be comprehended by the presence of vortex tubes, which are so-called quasistreamwise vortices. The tubelike

structures, which have been identified by the numerical simulation [1,2], are almost the same order of diameter as the quasistream vortices in wall-bounded shear flow. The longitudinal length scale seems to be 40–50 times the diameter because the inverse power-law region extends to fifty times the peak wave number k_p in Fig. 5.

We should also notice the exponential form of energy spectrum in the dissipation range ($5 \ll k/k_p$), which is reported by numerical simulations in isotropic flow [15,16]. In the near wall region, however, this exponential form is probably influenced by the quasistreamwise vortices; thus, this problem will be discussed in the next step of our research.

V. CONCLUSIONS

In the zero-pressure-gradient low Reynolds number ($R_\theta < 5000$) turbulent boundary layer, the peak locations of the shear stress profile and the energy dissipation spectrum were discussed. Based on the experimental data analysis, the peak position of the energy dissipation spectrum y_{kp}^+ is located very close to y_p^+ position. The distribution of y_{kp}^+ is scaled well by $y_{kp}^+ = 2R_*^{1/2}$, and the local mean velocity ratio is constant, $U(y_{kp}^+)/U_0 \simeq 0.62$.

ACKNOWLEDGMENTS

This work was performed during a stay at Yale University. The author is deeply grateful to Professor K. R. Sreenivasan for his hospitality, variable comments, and encouragement. Useful discussions with Dr. A. Sahay are much appreciated.

[1] J. Jiménez, A. A. Wray, P. G. Saffman, and R. S. Rogallo, J. Fluid Mech. **255**, 65 (1993).
[2] P. Passort, H. Politano, P. L. Sulem, J. R. Angiella, and M. Meneguzzi, J. Fluid Mech. **282**, 313 (1995).
[3] Z.-S. She and E. Jackson, Phys. Fluids A **5**, 1526 (1993).
[4] F. H. Champagne J. Fluid Mech. **86**, 67 (1978).
[5] V. Emsellem L. P. Kadanoff, D. Lohse, P. Tabeling, and Z. J. Wang, Phys. Rev. E **55**, 2672 (1997).
[6] P. S. Klebanoff, National Advisory Committee for Aeronautics Technical Note No. 3178, 1954 (unpublished).
[7] A. Honkan and Y. Andrepoulos, J. Fluid Mech. **350**, 29 (1997).
[8] J.-L. Balint, J. M. Wallace, and P. Vukoslavčević, J. Fluid Mech. **228**, 53 (1991).
[9] P. R. Spalart, J. Fluid Mech. **187**, 61 (1988).
[10] R. R. Long and T.-C. Chen, J. Fluid Mech. **105**, 19 (1981).
[11] K. R. Sreenivasan, in *Frontiers in Experimental Fluid Mechanics*, edited by Gad-el-Hak (Springer, Vienna, 1989), p. 159.
[12] R. L. Simpson J. Fluid Mech. **42**, 769 (1970).
[13] K. R. Sreenivasan has obtained more sensitive ratio, which is normalized by an inner variable as a function of Reynolds number.
[14] A. E. Perry and M. S. Chong, J. Fluid Mech. **119**, 173 (1982).
[15] S. Kida and Y. Murakami, Phys. Fluids **30**, 2030 (1987).
[16] R. M. Kerr J. Fluid Mech. **211**, 309 (1990).